Research Article

Investigation of an Air-Forced Open Cathode Proton Exchange Membrane Fuel Cell Stack Energy Efficiency with Different Fan Operation Mechanisms

Tan-Thich Do*
Department of Electrical and Mechatronics, Lac Hong University, Vietnam

Ngoc-Dang Nguyen
Ho Chi Minh City University of Science, Vietnam National University (HCMUS-VNU), Vietnam
Mechanical Engineering Department, National Chung Cheng University, Taiwan

* Corresponding author. E-mail: dotanthich@lhu.edu.vn
DOI: 10.14416/j.asep.2026.05.003
Received: 29 December 2025; Revised: 24 February 2026; Accepted: 20 March 2026; Published online: 12 May 2026

Abstract
The proton exchange membrane fuel cells (PEMFCs) are potential candidates for energy solutions toward net-zero emissions by 2050 owing to their remarkable properties. In the air-forced open cathode PEMFC stack (AF-OCPEMFCs), the electric fan was used to provide the air and dissipate the heat generated by the fuel cells. In this study, the performance and energy efficiency of the AF-OCPEMFCs were investigated under load levels and different fan mechanisms, including the blow and suction modes. The results show that the performance and energy efficiency of the blow mode are superior to the suction mode across the load levels, and the fan duty factors of 0.2, 0.4, 0.6, 0.8, and 1.0. Additionally, the hydrogen consumption was achieved at 0.014, 0.028, 0.042, and 0.056 L min^{-1}, corresponding to operating currents of 2, 4, 6, and 8 A, respectively. Notably, the highest energy efficiency was achieved at 35.04% under load levels of 6 A with blow mode. This study is meaningful for thermal management to optimize the energy efficiency of AF-OCPEMFCs for unmanned aerospace vehicles (UAVs) and electric vehicles (EVs).

Keywords: Air-forced open cathode, Electric vehicles, Energy efficiency, Fan speed, Hydrogen consumption, Proton exchange membrane fuel cells, Unmanned aerospace vehicles

1 Introduction

Nowadays, the proton exchange membrane fuel cells (PEMFC) are regarded as a promising energy solution owing to their significant characteristics, including zero-emission, low noise, low operation temperature, high energy efficiency, quick start, and high power density [1] among seven types of fuel cells [2]. Recently, it has been employed in a diversity of applications, such as portable power [3], station power [4], automobile [5], railway [6], ship [7], unmanned aerospace vehicles [8], and unmanned underwater vehicles [9]. Especially, the PEMFCs are attractive and more drawn in the context of many countries' commitment to achieving zero emissions by 2050 [10].

During the air-forced open cathode PEMFC stack (AF-OCPEMFCs) operation, it was affected by tremendous factors of operating conditions, such as key components, and materials, temperature, pressure, and humidity. For the affected key component and materials, Yeetsorn *et al.,* [11] studied the electrical conductivity of the bipolar plate for PEMFC. Their results showed that the external factor, including the pressure of clamping, affected the conductivity. Onyu *et al.,* [12] studied the electrical conductivity of the bipolar plates under varying materials. They revealed that the graphene agglomeration at a 7.5 wt% loading is a critical issue that must be addressed to improve volumetric electrical conductivity. Zhang *et al.,* [13] experimented to study the effect of a thermal radiation environment on the AF-OCPEMFCs' temperature and performance. They concluded that the stack voltage

was impacted by the thermal radiation, and the stack did not operate when high maximum radiation flux. Santa *et al.,* [14] analyzed the impact of ambient temperature and pressure on the power density of AF-OCPEMFCs with 8 cells. Their results show that at a power supply of 5 V for the fan voltage, the highest power density was achieved at 0.31 W cm^{-2} at a load density of 0.790 A cm^{-2}. Sagar *et al.,* [15] simulated to analyze the operational behavior of the performance of AF-OCPEMFCs. Their results indicated that the performance is better at high relative humidity and high-temperature ambient conditions. Ou *et al.,* [16] developed the bubble humidifier and control strategy of the humidified and temperature to increase the performance of AF-OCPEMFCs. They revealed that the stack performance increased by about 10% when using the bubble humidified and their control method. Barreras *et al.,* [17] examined the effect of pressure drop on the performance of AF-OCPEMFCs. Their results show that the measurement data and predicted data are in agreement with the friction factor in their study. Guilbert *et al.,* [18] analyzed a fuel cell boost converter and developed three adaptive Hamiltonian control laws, among which the third demonstrated superior performance.

To evaluate the effect of cathode components on the AF-OCPEMFCs, Zhao *et al.,* [19] designed and tested the channel of cathode flow for the AF-OCPEMFCs under varying dimension parameters. They optimized the cathode channel with a bipolar plate thickness of 2 mm and dimensions of bending angle (5°), width/landing (1:0.7), width (1.1 mm), and depth (1.3 mm), while Kreesaeng *et al.,* [20] researched the effect of the cathode channel on the AF-OCPEMFCs performance by using the computational method. Kiattamrong *et al.,* [21] examined the effect of airflow channels on the performance of the AF-OCPEMFCs. Their results show that the polarization curve under various airflow channels and compare them. This work was researched by Qiu *et al.,* [22] [23]. Wang *et al.,* [24] investigated electrochemical impedance spectroscopy (EIS) and voltage of the AF-OCPEMFCs under various cathode flow fields. Their results indicated that the cathode flow field with the metal foam is superior to another with the same testing conditions. The voltage improvement was also mentioned when placing metal foam in the channel of the cathode, which was reported [25]. Bujlo *et al.,* [26] developed and fabricated the AF-OCPEMFCs with 10 cells to test the performance. They indicated that the highest current density of 1200 mA cm^{-2} was achieved at a voltage of 0.5 V. Afterward, they tested durability with the long-term 300 h, and the voltage degradation of 0.64 mV h^{-1}. Zhao *et al.,* [27] experimented to examine the distribution of pressure on the AF-OCPEMFCs' performance. They concluded that the optimal compression ratio of the end plate of 70% to achieve maximum performance. Baik *et al.,* [28] developed cathode bipolar plates with a multi-hole framework to boost the performance of the AF-OCPEMFCs with 20 cells. They explained that the oxygen is uniform in multi-hole structures, leading to enhanced electrochemical performance, resulting in improved performance compared to conventional bipolar plate structures. Their works provided insightful methods. Kim *et al.,* [29] developed and designed the bipolar plates using the carbon composite. They have then optimized the stack sequence and thickness of bipolar plates. Chang *et al.,* [30] developed ultra-thin metal bipolar plates to examine the temperature distribution and voltage of the AF-OCPEMFCs. Their result revealed that the stack temperature should be uniform when the fuel cell is executed at high load levels.

For the material effect on the AF-OCPEMFCs, Liu *et al.,* [31] examined the performance of AF-OCPEMFCs under varying Pt/C, membranes, cathode catalyst layers, and cathode gas diffusion layers (GDLs). They indicated that the best performance was achieved at the composite Nafion/PTFE membrane with a thickness of 17 μm-thick. Zhao *et al.,* [32] tested the performance of the AF-OCPEMFCs under different GDLs and polytetrafluoroethylene (PTFE) content substrate layers. Their results show that the optimal GDL thickness and PTFE reached 200 μm and 10%.

In the AF-OCPEMFCs, the airflow rate was supplied by the electric fan. Additionally, the fan was used to dissipate the heat production from the stack owing to electrochemical reactions. The integration of the fan in the stack plays a significant role in optimizing the voltage of the stack [33]. Therefore, the stack performance and temperature were impacted by fan speed. Zeng *et al.,* [34] investigated the stack performance, uniform voltage, and temperature distribution under variable fan speeds at different load currents. They revealed that the fan speed dramatically affected the performance. Yu *et al.,* [35] investigated the self-regulating capability of the AF-OCPEMFCs under varying fan operations. They revealed that the suction mode is suitable for self-regulating capability

in their study. Ling *et al.,* [36] measured the stack temperature using the infrared camera and evaluated the stack voltage under air blow feed mode and air drawing feed mode. Their results revealed that the performance improved by 16% with the air-drawing feed mode. Yin *et al.,* [37] suggested a control strategy to optimize the thermal management in the AF-OCPEMFCs. They indicated that the system efficiency increased by 1% when using the constraint generalized predictive control (CGPC) and the highest efficiency optimization. Similarly, Yu *et al.,* [38] designed the control system and proposed a strategy in the AF-OCPEMFCs of 1000W to optimize thermal management using the CGPC technique. They concluded that the performance improved at the fan duty factor of 28.9% when compared to their proposal strategy and manufacture default strategy. D'Souza *et al.,* [39] studied the characteristics of thermal in a fuel cell stack with 80 cells using the numerical method. Their model provided insight into the thermal characteristics of a stack and indicated that the distribution of temperature affected the majority of stack performance. Mahjoubi *et al.,* [40] investigated and suggested a control strategy for the thermal management of the AF-OCPEMFCs. Their control strategy is appropriate in the stack because verified under various operating conditions. Zhou *et al.,* [41] studied the fan parameters on the performance of the AF-OCPEMFCs under various fan models, such as size, fan power, weight, and air volume. They indicated that the selection of the fan parameters impacts the AF-OCPEMFCs. Zhang *et al.,* [42] examined the impact of a fan on the performance of the AF-OCPEMFCs under varying parameters such as fan blade, morphology, and grill using the three-dimensional (3D) model. They revealed that the distribution of stack temperature and voltage in each cell is not uniform.

In summary, the AF-OCPEMFCs' performance and temperature were affected by the airflow rate. As we all know, the thermal management in AF-PEMFCs plays a crucial role, which affected significant to the output voltage and energy efficiency. Because the open-cathode PEMFC stack used the electric fan to fed the air and cool the heat generation, which is generated from the electrochemical reaction. Therefore, this study aims to find the optimal electric fan mechanism by investigating under various fan duty factors, which are represented by the fan speed and fan-mode, including blow mode and suction mode, that play an important role in the system. Although the performance of the AF-OCPEMFCs has been researched. There are a few studies on the impact of fan speed on stack performance; however, understanding the effect of fan speed under various fan duty factors and fan modes plays a crucial role in optimizing thermal management to extend the fuel cell stack lifespan. Although several studies indicated the suction mode is better than the blow mode [43], [44], performance depends on the quality of the fuel cell stack, fuel cell stack type, fuel cell stack characteristics, specific applications, and operating conditions. This is indicated last reported in [45], the blow mode is superior to the suction mode. To determine the best fan mode in the AF-OCPEMFCs 100 W, 20 cells in this study, the energy efficiency was investigated under varying fan operation mechanisms, including the blow mode, suction mode, and fan duty factors at different load levels. The energy efficiency between the blow mode and suction mode was compared, and indicated that the blow mode is superior to the suction mode across load levels and fan duty factors in this study. Because of the high pressure in the stack and stack temperature improvement when using the blow mode, leading to improved energy efficiency. This study is meaningful for managing the airflow rate and thermal in the stack of 100 W, 20 cells for UAVs.

2 Experimental

2.1 *Experimental setup*

Figure 1 depicts the real picture of the hardware experimental and experimental setup schematic, which comprised a hydrogen-supplied system, an open-cathode PEMFC stack, ancillary devices, and measurement equipment in this study. The AF-OCPEMFCs were purchased from the manufacturer (H-100 PEM, Horizon, USA) and employed to investigate the energy efficiency under various electric fan mechanisms. The specifications were summarized in Table 1 [46]. To reduce the degradation of the membrane, the AF-OCPEMFCs operated with the operating current load levels ranging from 2 to 8 A, with an increment of 2 A in this study. At the inlet anode side, the pure dry hydrogen (99.999%) was provided to the AF-OCPEMFCs via a pressure regulator (R06-221-NNEA, Norgren, Mexico), which was used to reduce and maintain anode pressure around 0.45 bar. The hydrogen supply valve was placed to prevent hydrogen gas leakage

when the system shuts down. The hydrogen flow rate meter (M-10 SLPM-D/5 M, Alicat Scientific, USA) was employed to determine the hydrogen consumption during the AF-OCPEMFCs operation. To save and enhance the hydrogen utilization, the solenoid valve, which was called the purge valve, was used to block the hydrogen gas at the anode outlet. Also, the purge valve was open to expel the gas and impurities when it received the control signal. The electric axial fan was utilized to provide the air and dissipate the heat generated by the fuel cells. The microcontroller unit (MCU) was designed and fabricated to control the fan speed, hydrogen supply valve, and purge valve. The control program was conducted in the MATLAB/Simulink software and deployed in the microcontroller unit (MCU).

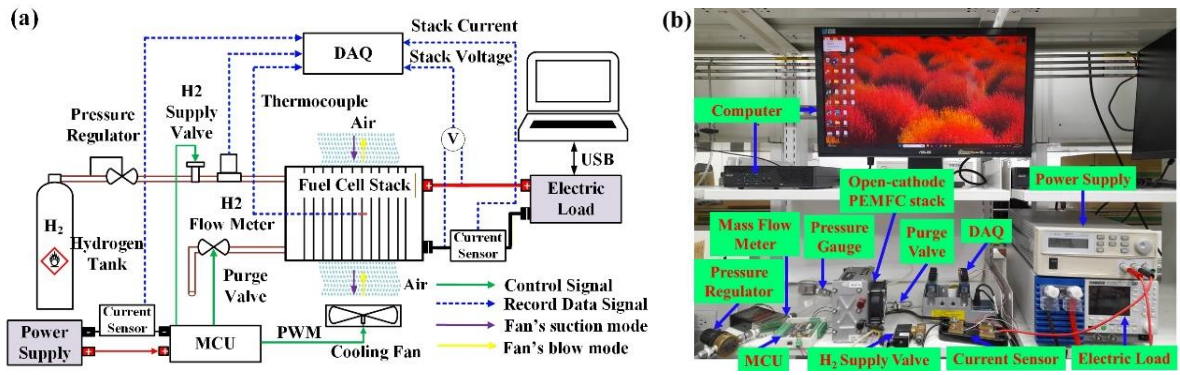

Figure 1: Experimental setup scheme of AF-OCPEMFCs system (a); A real picture of hardware for this study (b).

Table 1: Key specifications of AF-OCPEMFCs.

Parameter	Value
Membrane type	PEMFC
Number of cells	20
Size (height x length x width) /mm	94×104×118
Cell activation area / cm^2	22.5
Rated power / W	100
Weight of stack / g	1290 (±) 50
Gas cathode side	Air
Hydrogen purity / %	99.99

The direct current (DC) power supply machine (U8001A, Keysight, USA) was used to provide the power source for auxiliary equipment, such as an electric fan, purge valve, hydrogen supply valve, and MCU. To measure the temperature of the fuel cell, the thermocouple (WTC-TT-T-36, IOThrifty, USA) was employed and placed in the center of the stack. The shunt current (SH-0010A-50mV, CPU Co., Ltd, Taiwan) was utilized to measure the auxiliary current and operating current during fuel cell stack operation. The electric load (PLZ164WA, Kikusui, Japan) was used to apply the electrical load levels for the fuel cell stack. Ultimately, the data acquisition (DAQ) (NI 9219, National Instruments, USA) was used to collect real-time signals, including the hydrogen mass flow rate, stack voltage, stack temperature, stack current, and auxiliary current.

2.2 *Experimental procedure*

Figure 2 shows the flowchart of experimental procedures for this study, including the fuel cell stack activation process and experimental investigation process of the electric fan operation mechanisms in AF-OCPEMFCs system. The AF-OCPEMFCs operated at the ambient condition with the room temperature of 25 °C, and pressure of 1 atm.

The fuel cell stack has undergone an activation process of around 1 hour at load levels of 4 A before conducting an experiment. This activation process aims to achieve a stable performance of the AF-OCPEMFCs by a humidified membrane [47]. Afterward, the control purge valve was operated in a continuous open–close cycle to remove water and impurities until none remained.

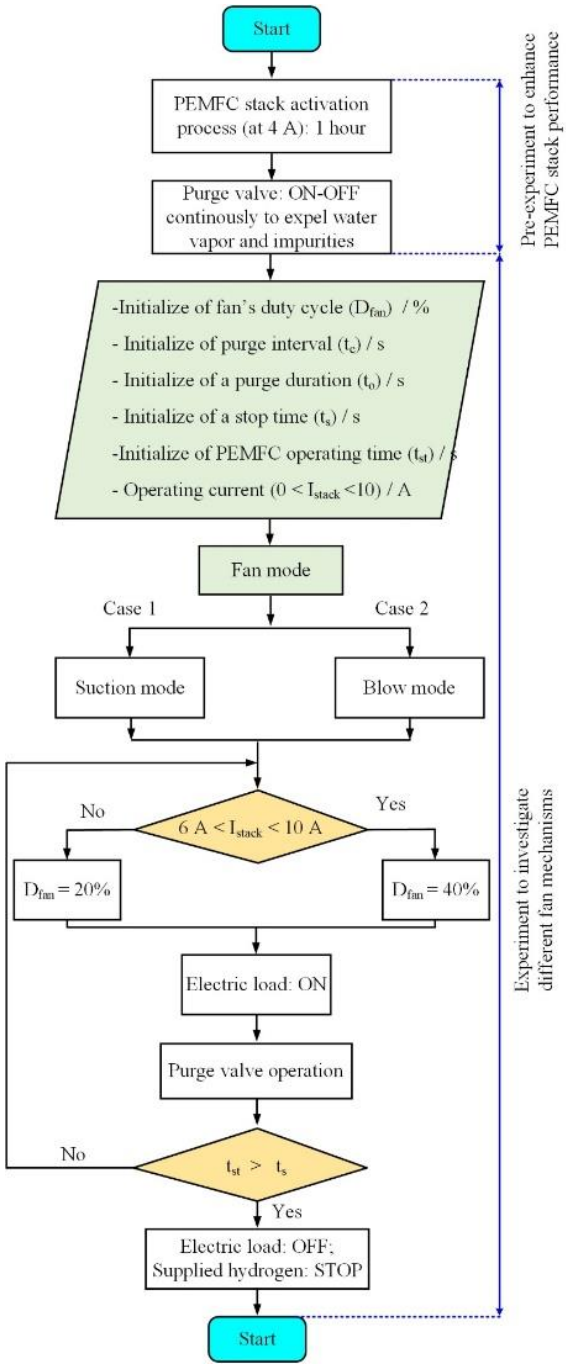

Figure 2: Flowchart of experimental procedures for this study.

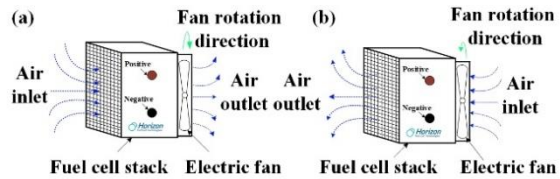

Figure 3: Illustration of an electric fan operation mechanism in the AF-OCPEMFCs system: Suction mode (a); Blow mode (b).

In this study, the effect of operating temperature on the voltage of AF-OCPEMFCs was examined at current levels of 2, 4, 6, and 8 A, with fan duty factors of 0.2, 0.4, 0.6, 0.8, and 1.0, and under two fan mechanisms: suction and blow modes, as shown in Figure 3. The pulse width modulation (PWM) technique was deployed to control the electric fan speed. Additionally, the fan duty factor was determined as follows:

$$D_{fan} = \frac{PW}{T_{period}} \tag{1}$$

where: PW is the time of pulse activity, and T_{period} is the total signal period. Obviously, a higher fan duty factor higher flow rate.

During the AF-OCPEMFCs operation, the energy efficiency (η) was evaluated under various load levels and fan duty factors. The energy efficiency in this study was calculated using Equation (2)

$$\eta = \frac{60 \times 22.4 \int P_{net}(t)dt}{LHV \int \dot{m}_{H_2}(t)dt} = 60 \times 22.4 \left[\frac{\left(I_{fcs}\sum_i V_{fcs}(i) - I_{anc}\sum_i V_{anc}(i)\right)\Delta t}{LHV \sum_i \dot{m}_{H_2}(i)\Delta t}\right] \tag{2}$$

where: P_{net}, LHV, and $\dot{m}_{H_2}$ refer to the net power output, in W; hydrogen's lower heating value [48], ($LHV = 242 \times 10^3 \text{J mol}^{-1}$); and hydrogen mass flow rate, in liters per second (L s^{-1}), respectively. Additionally, I_{fcs} is the operating stack current, in A; V_{fcs} denotes the fuel cell stack voltage, in V ; I_{anc} refers to the current of ancillary equipment, in A, and i represents the summation index. The net power output depended on the power of the AF-OCPEMFCs and the power of the ancillary. It was determined using Equation (3):

$$P_{net} = P_{fcs} - P_{anc} \tag{3}$$

where: P_{fcs} is the power of the AF-OCPEMFCs, and P_{anc} is the power of ancillary, including the power consumption of the hydrogen-supplied valve, fan, purge valve, and MCU. All parameters are units of W.

The power of the AF-OCPEMFCs depended on the current and voltage of the stack. It can be determined as follows:

$$P_{fcs} = V_{fcs} \times I_{fcs} \quad (4)$$

For the power of ancillary, a lower ancillary power is better, because a higher net power output leads to high energy efficiency in this study. The power of ancillary can be calculated by Equation (5):

$$P_{anc} = V_{anc} \times I_{anc} = P_{hsv} + P_{elf} + P_{pv} + P_{MCU} \quad (5)$$

where: P_{hsv}, P_{elf}, P_{pv}, and P_{MCU} denote the power of the hydrogen supplied valve, in W; power of the electric fan, in W; power of the purge valve, in W; and power of the MCU, in W, respectively.

To eliminate the water, impurities, and nitrogen accumulation at the anode channel, the purge valve was opened with a purge duration of 100 ms and a purge interval of 20 s. It aims to recover the stack performance by changing the fresh hydrogen.

3 Results and Discussion

3.1 *Effect of electric fan duty factor on stack performance*

During the AF-OCPEMFCs operation, the fan speed influenced the stack voltage. In this section, the blow mode was used to discuss the impact of the fan duty factor under varying load levels. Figure 4 depicts the variation of the voltage and temperature of the AF-OCPEMFCs under various operating currents. At the low operating current of 2 A, the voltage seems stable and remains constant after applying the load, as shown in Figure 4(a). In this load, water and heat generation from the stack were low, while the purge valve was opened frequently and was removed. The stack temperature was low owing to the low current, and almost all the heat generation was dissipated by the electric fan, as described in Figure 4(b). At the stable temperature, the maximum temperature was achieved at 35 °C for the fan duty factor of 0.2. When the current is elevated to 4 A, the voltage is lower than 2 A due to an overpotential increase. When applying the current, the stack of fuel cells tended to gradually increase, as described in Figure 4(c). This phenomenon can be elucidated by the rate of electrochemical reaction that occurred at a rate higher than the current of 2 A, leading to more heat generation to enhance the membrane, resulting in voltage improvement. In addition, the temperature of the AF-OCPEMFCs gradually increased from the temperature of the laboratory room to the stable temperatures of 60, 40, 30, 29, and 25 °C corresponding to the electric fan duty factors of 0.2, 0.4, 0.6, 0.8, and 1.0, as described in Figure 4(d). The electrochemical reaction rate in this load was higher than 2 A, resulting in more heat generation. When the electric fan duty factor increased, the temperature of AF-OCPEMFCs decreased because the higher fan duty factor resulted in a higher airflow rate. Therefore, a larger amount of heat was removed from the stack.

When the AF-OCPEMFCs operated at a current of 6 A, the voltage gradually increased and achieved a stable. It is noteworthy that the maximum voltage of 12.3 V occurred at the electric fan duty factor of 0.2 due to the low fan duty factor, and the voltage was reduced stratification as the fan duty factor increased, as shown in Figure 4(e). It can be elaborated that the amount of heat generation from the electrochemical reaction enhanced the membrane conductivity. When the fan duty factor increased, the temperature of the AF-OCPEMFCs decreased because the heat generated was eliminated when the electric fan speed increased, as represented in Figure 4(f).

At the high load of 8 A, the performance of AF-OCPEMFCs was profoundly influenced by the fan duty factors, as described in Figure 4(g). The voltage gradually increased after applying load current and dropped rapidly at 430th second for the fan duty factor of 0.2. This phenomenon can be explained by the fact that the heat generated was high while the fan speed was low. Therefore, the provided airflow rate is insufficient for the stack's electrochemical reaction. Additionally, more heat generation could not dissipate, leading to a dry membrane, resulting in a rapid stack voltage drop. However, when the fan duty factor increased to 0.4, 0.6, 0.8, and 1.0, the stack voltage was stable and achieved at 12, 13, 14, and 15 V for the fan duty factors of 0.4, 0.6, 0.8, and 1.0, respectively. It was observed that heat removal was more effective at higher fan duty factors than at a low fan duty factor of 0.2, leading to improved stack performance. Therefore, when the load current increases, the fan speed should be increased to adapt to the provided amount of airflow rate and dissipate

heat. In this load, the maximum voltage of 15 V was achieved at the fan duty factor of 0.4. Obviously, the stack temperature decreased when the electric fan duty factor increased owing to more heat generation removal, as shown in Figure 4(h).

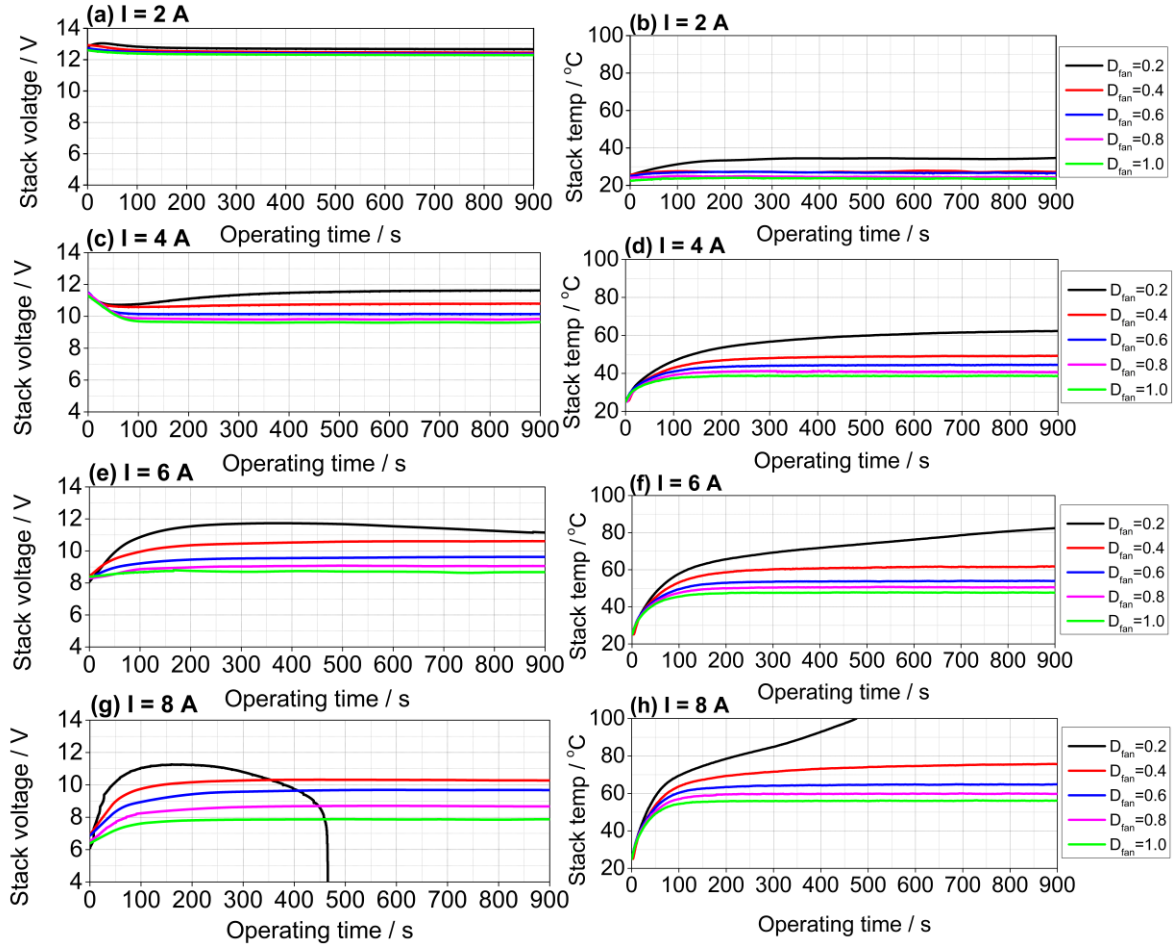

Figure 4: Variation of the voltage and temperature of the AF-OCPEMFCs under varying fan duty factors and currents: 2 A (a–b); 4 A (c–d); 6 A (e-f); and 8 A (g–h).

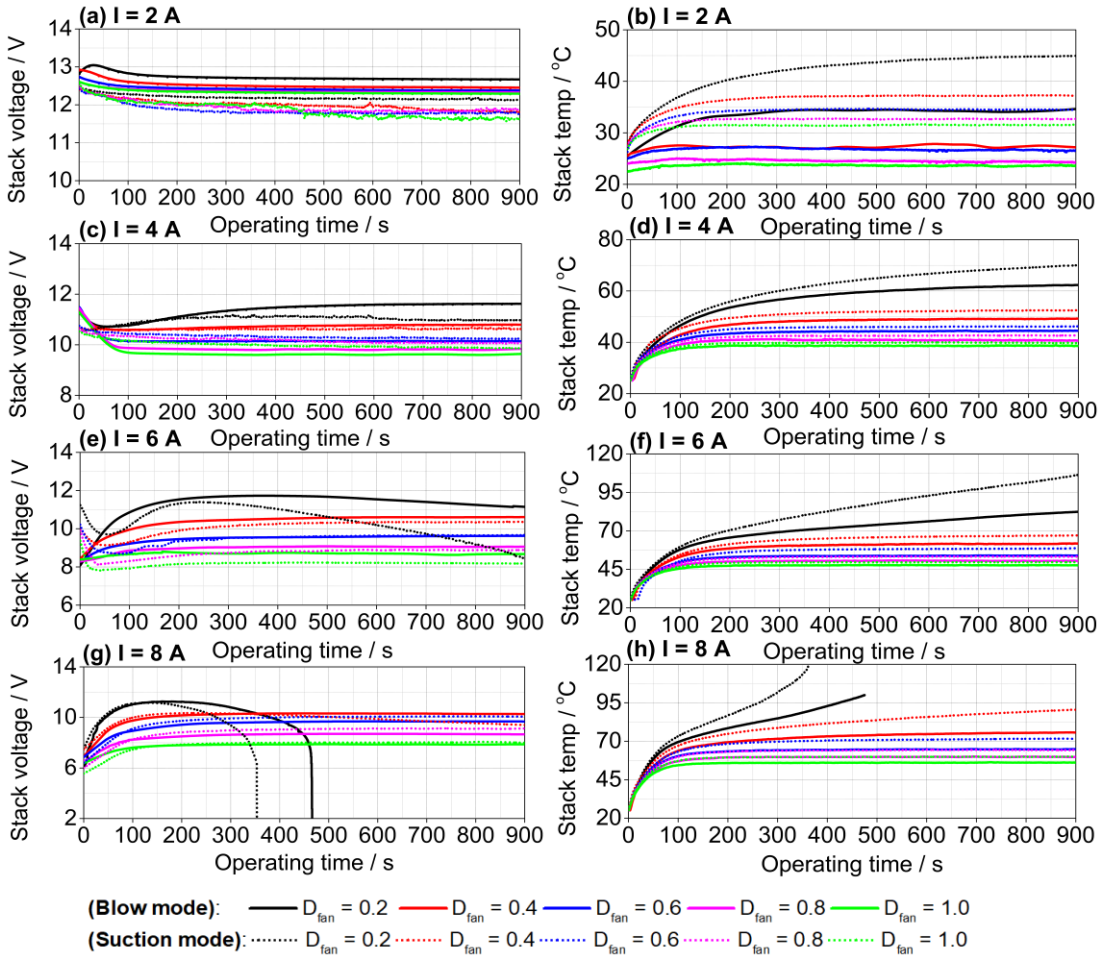

Figure 5: Comparison of the voltage and temperature of the AF-OCPEMFCs under varying fan duty factors and currents: 2 A (a–b); 4 A (c–d); 6 A (e-f); and 8 A (g–h).

3.2 *Effect of fan blow mode and fan suction mode on stack performance*

In this study, the voltage of the AF-OCPEMFCs was investigated under different fan mechanisms, including the blow mode and suction mode. Therefore, it should be compared to find the best mode for the open-cathode PEMFCs of 100 W. Figure 5 shows the stack performance and stack temperature under varying load current and fan duty factors for the blow mode and suction mode. It is noticeable that the voltage of the stack with blow mode is superior to suction mode across load level, as depicted in Figure 5(a), (c), (e), and (g). In other words, the voltage stack was improved for the blow mode. This can be explained by the fact that the blow mode provided an airflow rate better than the suction mode because the blow mode generated high pressure in the fuel cell stack. It was also the last report in [45].

In the blow mode, the heat generation from the electrochemical reaction of a stack was removed better than the suction mode owing to the higher airflow rate in the blow mode. Thus, the AF-OCPEMFCs temperature in blow mode is lower than in suction mode. The blow mode is the best choice for improving the voltage of the stack and ensuring good dissipation of heat.

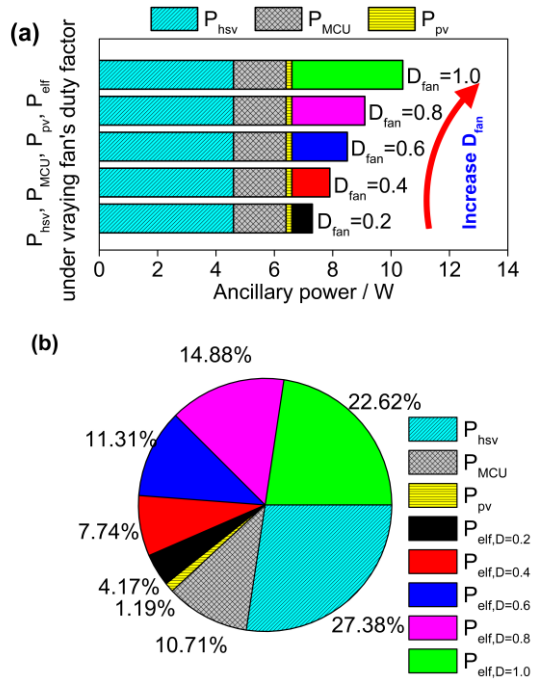

Figure 6: Ancillary power under varying fan duty factors (a); Percentage of ancillary power (b).

3.3 *Analysis of ancillary power and hydrogen consumption under load levels*

The energy efficiency of the AF-OCPEMFCs depended on the ancillary power and hydrogen consumption for electrochemical reactions. Notably, the electric fan speed contributes significantly to the ancillary power. Indeed, when the fan duty factor increases, that means a higher airflow rate is provided to the AF-OCPEMFCs, resulting in the power consumption of ancillary increased. On the other hand, the power of ancillary consumption consisted of the power consumption of the hydrogen supply valve, the MCU, and the purge valve. The ancillary power consumption and the percentage of ancillary power consumption in this study are described in Figure 6. It is apparent that the contribution of electric fan power consumption was higher when the fan duty factor increased. The percentage of electric fan power increased by 4.17%, 7.74%, 11.31%, 14.88%, and 22.62% corresponding to fan duty factors of 0.2, 0.4, 0.6, 0.8, and 1.0. Obviously, the fan speed increased, and the airflow rate increased, resulting in reduced local overheating [49] and stack voltage uniformity in each cell in the stack [50]; however, the membrane can be dehydrated. The higher fan speed leads to increased ancillary power, resulting in reduced energy efficiency [51], while the low fan speed leads to insufficiency of airflow rate or overheating of the stack at high load operation. Therefore, the electric fan speed must not be controlled without consideration. It should be optimized according to the load level. The fan duty factor in this study was found to be 20% for low and medium load levels less than 6 A. For the load levels beyond that point, the fan duty factor was 40%. Because the fuel cell stack needs a higher airflow rate at high load levels. Additionally, the heat produced by the electrochemical reactions in the AF-OCPEMFCs should be removed to maintain the stack temperature. It aims to prevent dry membranes and enhance performance.

The hydrogen consumption should be considered during the AF-OCPEMFCs operation. The hydrogen consumption depended on the significant load levels of the AF-OCPEMFCs. As the operating load levels increased, the hydrogen consumption ($V_{H2\ cons}$), in litters per minute (LPM), increased to serve the electrochemical reactions and was determined as follows:

$$V_{H2\ cons} = \frac{N_{cell} \times I}{2F} \times 60 \times 22.4 \tag{6}$$

where: N_{cell} denotes the cell number in a stack, I is the operating current, and F represents the Faraday's constant.

To save and enhance hydrogen utilization, the dead-end anode mode was employed in this study. The optimization of hydrogen consumption is a key factor. The optimization duration of the purge valve opened and closed time status will be investigated in the future. In this study, the purge interval, representing the time the purge valve remains closed, was set to 20 s. The purge duration, or the time the purge valve stays open, was 100 ms. When the solenoid valve opened, gas was evacuated from the anode channel. The gas volume flow rate, in LPM, can be calculated using Equation (7):

$$\dot{V} = \frac{5140}{3600} \times K_v \times \sqrt{p_0 \frac{(p_a - p_0)}{T\rho}} \tag{7}$$

where: K_v, p_0, p_a, T, and ρ represent the purge valve's characteristic value, outlet pressure when the purge

valve opens, anode pressure, stack temperature, and gas density, respectively.

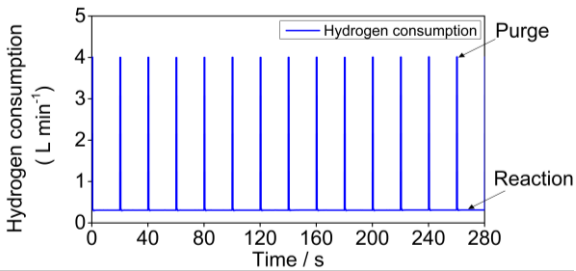

Figure 7: Hydrogen consumption during the stack operation.

Figure 7 shows the hydrogen consumption flow rate for the electrochemical reactions of the AF-OCPEMFCs and the purged gas volume flow rate during the purge valve opening. It can be observed that when the load level increased, the hydrogen consumption flow rate for the electrochemical reaction during the dead-end anode mode was achieved at 0.014, 0.028, 0.042, and 0.056 L min^{-1} corresponding to load levels of 2, 4, 6, and 8 A. When the purge valve opened, the unreacted hydrogen was purged to the atmosphere, leading to rapidly increased the volume flow rate and achieved at 4.04 L min^{-1}. The unreacted hydrogen was expelled to the outside, which was called wasted hydrogen, and the duration of the purge valve opening was determined in the future. In this study, the optimization of the electric fan was conducted, thus the purge interval and purge duration were fixed.

3.4 *Discussion on energy efficiency between blow mode and suction mode*

Energy efficiency is a key parameter to elucidate the effectiveness of the open-cathode PEMFC stack, including the power output and hydrogen consumption. In this study, the energy efficiency was determined and evaluated under various fan mechanisms and load levels. The energy efficiency for the blow mode and suction mode is shown in Figures 8(a) and (b), respectively. In the blow mode, it is noticeable that at load levels 2, 4, and 6 A, the energy efficiency gradually decreased when the fan duty factor increased. This can be explained by more ancillary power consumption when the fan duty increases, contributing to reducing the net power output following Equation (3). The maximum energy efficiency was achieved at the electric fan duty factor of 0.2 for the load levels of 2, 4, and 6 A. When the AF-OCPEMFCs operated at a load level of 8 A, the maximum energy efficiency was achieved at the electric fan duty factor of 0.4, because a high load level of 8 A needs a larger amount of airflow to provide and adapt to the electrochemical reactions of the fuel cell stack. Additionally, a higher airflow rate dissipates the heat generation from the stack increase, leading to the electric fan duty factor being increased to 0.4. The highest energy efficiency of 35.04% at a load level of 6 A with the fan duty factor of 0.2 for the blow mode.

For the suction mode, the energy efficiency of the AF-OCPEMFCs under load levels of 2, 4, 6, and 8 A and varying fan duty factors of 0.2, 0.4, 0.6, 0.8, and 1.0, as described in Figure 8(b). It is clear that when the fan duty factor increased, the energy efficiency gradually decreased due to the higher fan duty factor leading to higher ancillary power consumption, resulting in reduced net power output. Indeed, energy efficiency seems to reduce linearly when the fan duty factor increases. For a load level of 2 A, the energy efficiency was achieved at 26.11%, 24.60%, 23.63%, 23.59%, and 21.73%, corresponding to the fan duty factors of 0.2, 0.4, 0.6, 0.8, and 1.0. Similarly, the reduction of energy efficiency linearly was achieved at 30.05%, 28.41%, 27.22%, 26.51%, and 25.56% corresponding to the fan duty factors of 0.2, 0.4, 0.6, 0.8, and 1.0. For the operating load level of 6 A, the energy efficiency gradually decreased by 32.48%, 31.32%, 28.38%, 25.86%, and 23.57%, corresponding to the fan duty factors of 0.2, 0.4, 0.6, 0.8, and 1.0. Notably, the energy efficiency was achieved at the lowest of 23.15% at the electric fan duty factor of 0.2 with a load level of 8 A. It can be explained that the fan speed was low, leading to an insufficient airflow rate, while the higher load level needed a higher airflow rate to provide for the electrochemical reactions of the stack. Additionally, high heat generation from the fuel cell caused a dry membrane, reducing the surface area of the catalyst and mass transport limitation, resulting in reduced performance [52], [53]. The stack voltage was dropped rapidly at 500 s at a high level of 8 A, which was explained in detail in sections 3.1 and 3.2. Therefore, a higher load level should result in a higher fan duty factor. At a high load level of 8 A, the highest energy efficiency was achieved 31.08% because of insufficient airflow rate and low ancillary power consumption.

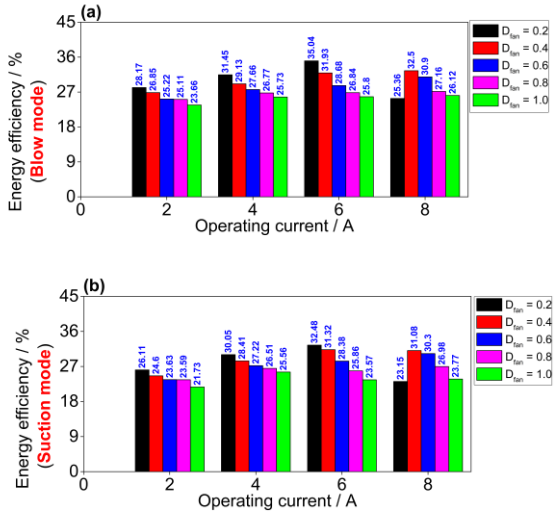

Figure 8: Energy efficiency of the AF-OCPEMFCs under various fan duty factors, and load levels for blow mode (a), and suction mode (b).

To compare the energy efficiency of the blow mode and suction mode, the energy efficiency was listed under varying load levels and fan duty factors with the blow mode and suction mode, as depicted in Table S1 (in Supplementary Materials). It can be seen that the energy efficiency with blow mode is superior to suction mode across load levels and the fan duty factors. This is because the stack voltage and stack temperature with the blow mode are better than those with the suction mode.

3.5 Capability configuration for applications

In this study, the performance and energy efficiency of AF-OCPEMFCs were investigated under different fan mechanisms. The AF-OCPEMFCs use an electric fan to supply oxygen from the ambient air. Therefore, this configuration features a simple system architecture and an easier control strategy. Since the AF-OCPEMFCs operate under ambient conditions with an excess air supply, this configuration is suitable not only for UAV applications but also for electric vehicles (EVs) applications. Figure 9 depicts the AF-OCPEMFCs applied in EVs. It can be observed that the traction system is powered by the AF-OCPEMFCs. EVs that rely solely on AF-OCPEMFCs as the main power source are referred to as pure fuel cell electric vehicles or full fuel cell electric vehicles (full FCEVs) [54].

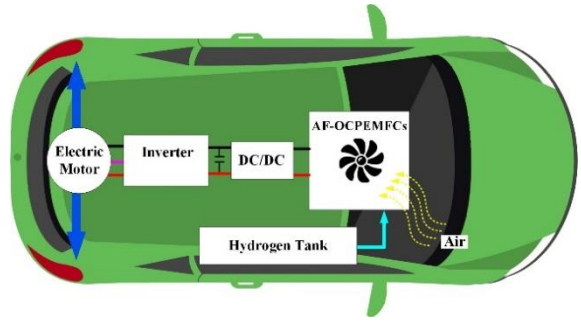

Figure 9: AF-OCPEMFCs in full FCEVs.

4 Conclusions

The voltage and energy efficiency of the AF-OCPEMFCs were investigated under various load currents and fan operation mechanisms, including the blow mode, suction mode, and different fan duty factors. The results obtained from the experiment are explained in the previous sections. Several highlighted were drawn following the statements:

(1) When the electric fan duty factor increased, the temperature of the AF-OCPEMFCs reduced because the heat generated by electrochemical reactions was removed.

(2) When the load current increased, the voltage decreased owing to increasing water and impurities, leading to an increase in the overpotential. In addition, the stack temperature increased owing to the increasing heat produced from the electrochemical reactions of the AF-OCPEMFCs.

(3) The energy efficiency of the AF-OCPEMFCs with the blow mode is superior to the suction mode across load levels and the fan duty factors.

(4) At a high load level, the voltage was improved because the temperature of the AF-OCPEMFCs with blow mode was lower than with suction mode. This cause is heat-generated removal with high-pressure blow mode.

(5) Because the AF-OCPEMFCs operated in the ambient with the air, and used the electric fan to feed the oxygen from the air. Thus, this configuration is appropriate for UAVs and EVs.

In this study, the optimal electric fan mechanism was identified by varying the fan duty factor, which represents the fan speed, as well as the electric fan operating modes, including suction and blowing modes. In future work, a thermal management strategy using an intelligent control algorithm is proposed to further optimize the electric fan mechanism.

Acknowledgments

During the conduct of this study, the first author would like to thank Lac Hong University for financial support. The last author is grateful to the Department of Mechanical Engineering, National Chung Cheng University, and the Taiwan Experience Education Program (TEEP), Taiwan, Republic of China (R.O.C.), for supporting this study.

Author Contributions

T.T.D.: conceptualization, investigation, reviewing and editing, funding acquisition, project administration, writing an original draft, writing—reviewing and editing; N.D.N.: investigation, methodology, writing an original draft, research design, data analysis, data curation. All authors have read and agreed to the published version of the manuscript.

Conflicts of Interest

The authors declare no conflict of interest.

Declaration of generative AI and AI-assisted technologies in the writing process

The authors have not utilised any generative AI tool for any assistance in the writing process.

Supplementary Materials

The supplementary materials can be found: DOI: https://doi.org/10.17632/22w4pcwh8x.2.

References

[1] F. Barbir, *PEM fuel cells: theory and practice*. Massachusetts: Academic Press, 2012.

[2] F. M. Guangul and G. T. Chala "A comparative study between the seven types of fuel cells," *Applied Science and Engineering Progress*, vol. 13, no. 3, pp. 185–194, 2020, doi: 10.14416/j.asep.2020.04.007.

[3] Y.-J. Sohn *et al.,* "Operating characteristics of an air-cooling PEMFC for portable applications," *Journal of Power Sources*, vol. 145, no. 2, pp. 604–609, 2005, doi: 10.1016/j.jpowsour.2005.02.062.

[4] S. J. C. Cleghorn *et al.,* "PEM fuel cells for transportation and stationary power generation applications," *International Journal of Hydrogen Energy*, vol. 22, no. 12, pp. 1137–1144, 1997, doi: 10.1016/S0360-3199(97)00016-5.

[5] A. Mohammadi *et al.,* "Diagnosis of PEMFC for automotive application," in 2015 5th International Youth Conference on Energy (IYCE), 2015, doi: 10.1109/IYCE.2015.7180793.

[6] J. Lee *et al.,* "Empirical lifetime prediction through deterioration evaluation of high-power PEMFC for railway vehicle applications," *International Journal of Hydrogen Energy*, vol. 71, pp. 972–981, 2024, doi: 10.1016/j.ijhydene.2024.05.185.

[7] K. M. Bagherabadi, S. Skjong, and E. Pedersen, "Dynamic modelling of PEM fuel cell system for simulation and sizing of marine power systems," *International Journal of Hydrogen Energy*, vol. 47, no. 40, pp. 17699–17712, 2022, doi: 10.1016/j.ijhydene.2022.03.247.

[8] D. Zhao *et al.,* "Design and control of air supply system for PEMFC UAV based on dynamic decoupling strategy," *Energy Conversion and Management*, vol. 253, 2022, Art. no. 115159, doi: 10.1016/j.enconman.2021.115159.

[9] Y. Liu, J. Zhao, and Z. Tu, "Detecting performance degradation in a dead-ended hydrogen-oxygen proton exchange membrane fuel cell used for an unmanned underwater vehicle," *Renewable Energy*, vol. 222, 2024, Art. no. 119950, doi: 10.1016/j.renene.2024.119950.

[10] H. N. Khokhar, "Decarbonisation of global economies; is net zero emission achievable? The case for hydrogen and fuel cell technology for innovative futures," *Journal of Entrepreneurship and Innovation in Emerging Economies*, vol. 9, no. 1, pp. 92–130, 2023, doi: 10.1177/23939575221141578.

[11] R. Yeetsorn and M. Fowler, "Resistance measurement of conductive thermoplastic bipolar plates for polymer electrolyte membrane fuel cells," *Applied Science and Engineering Progress*, vol. 7, no. 4, pp. 13–21, 2014, doi: 10.14416/j.ijast.2014.08.001.

[12] K. Onyu *et al.,* "Evaluation of the possibility for using polypropylene/graphene composite as bipolar plate material instead of polypropylene/graphite composite," *Applied*

Science and Engineering Progress, vol. 9, no. 2, pp. 99–111, 2016, doi: 10.14416/j.ijast.2016.02.003.

[13] J. Zhang, C. Wang, and A. Zhang, "Experimental study on temperature and performance of an open-cathode PEMFC stack under thermal radiation environment," *Applied Energy*, vol. 311, Art. no. 118646, 2022, doi: 10.1016/j.apenergy.2022.118646.

[14] D. T. S. Rosa *et al.,* "High performance PEMFC stack with open-cathode at ambient pressure and temperature conditions," *International Journal of Hydrogen Energy*, vol. 32, no. 17, pp. 4350–4357, 2007, doi: 10.1016/j.ijhydene.2007.05.042.

[15] A. Sagar *et al.,* "A computational analysis on the operational behaviour of open-cathode polymer electrolyte membrane fuel cells," *International Journal of Hydrogen Energy*, vol. 45, no. 58, pp. 34125–34138, 2020, doi: 10.1016/j.ijhydene.2020.09.133.

[16] K. Ou *et al.,* "Performance increase for an open-cathode PEM fuel cell with humidity and temperature control," *International Journal of Hydrogen Energy*, vol. 42, no. 50, pp. 29852–29862, 2017, doi: 10.1016/j.ijhydene.2017.10.087.

[17] F. Barreras *et al.,* "Experimental study of the pressure drop in the cathode side of air-forced open-cathode proton exchange membrane fuel cells," *International Journal of Hydrogen Energy*, vol. 36, no. 13, pp. 7612–7620, 2011, doi: 10.1016/j.ijhydene.2011.03.149.

[18] D. Guilbert *et al.,* "Comparative study of adaptive Hamiltonian control laws for DC microgrid stabilization: A fuel cell boost converter," *Applied Science and Engineering Progress*, vol. 15, no. 3, 2022, Art. no. 5540, doi: 10.14416/j.asep.2021.10.005.

[19] C. Zhao *et al.,* "Optimal design of cathode flow channel for air-cooled PEMFC with open cathode," *International Journal of Hydrogen Energy,* vol. 45, no. 35, pp. 17771–17781, 2020, doi: 10.1016/j.ijhydene.2020.04.165.

[20] S. Kreesaeng, B. Chalermsinsuwan, and P. Piumsomboon, "Effect of channel designs on open-cathode PEM fuel cell performance: A computational study," *Energy Procedia*, vol. 79, pp. 733–745, 2015, doi: 10.1016/j.egypro.2015.11.559.

[21] S. Kiattamrong and A. Sripakagorn, "Effects of the geometry of the air flowfield on the performance of an open-cathode PEMFC—transient load operation," *Energy Procedia*, vol. 79, pp. 612–619, 2015, doi: 10.1016/j.egypro.2015.11.541.

[22] D. Qiu *et al.,* "Numerical analysis of air-cooled proton exchange membrane fuel cells with various cathode flow channels," *Energy*, vol. 198, 2020, Art. no. 117334, doi: 10.1016/j.energy.2020.117334.

[23] B. Kim *et al.,* "Effects of cathode channel size and operating conditions on the performance of air-blowing PEMFCs," *Applied Energy*, vol. 111, pp. 441–448, 2013, doi: 10.1016/j.apenergy.2013.04.091.

[24] Z. Wang *et al.,* "Operation characteristics of open-cathode proton exchange membrane fuel cell with different cathode flow fields," *Sustainable Energy Technologies and Assessments*, vol. 49, 2022, Art. no. 101681, doi: 10.1016/j.seta.2021.101681.

[25] D. G. Kang *et al.,* "Performance enhancement of air-cooled open cathode polymer electrolyte membrane fuel cell with inserting metal foam in the cathode side," *International Journal of Hydrogen Energy*, vol. 45, no. 51, pp. 27622–27631, 2020, doi: 10.1016/j.ijhydene.2020.07.102.

[26] P. Bujlo *et al.,* "Development, manufacture and validation of an open cathode LT-PEMFC stack at HySA systems," *International Journal of Hydrogen Energy*, vol. 46, no. 57, pp. 29478–29487, 2021, doi: 10.1016/j.ijhydene.2020.11.235.

[27] C. Zhao *et al.,* "An experimental study on pressure distribution and performance of end-plate with different optimization parameters for air-cooled open-cathode LT-PEMFC," *International Journal of Hydrogen Energy*, vol. 45, no. 35, pp. 17902–17915, 2020, doi: 10.1016/j.ijhydene.2020.04.270.

[28] K. D. Baik and S. H. Yang, "Improving open-cathode polymer electrolyte membrane fuel cell performance using multi-hole separators," *International Journal of Hydrogen Energy*, vol. 45, no. 15, pp. 9004–9009, 2020, doi: 10.1016/j.ijhydene.2020.01.040.

[29] M. Kim, "Optimum design of the carbon composite bipolar plate for the open cathode of an air-breathing PEMFC," *Composite*

Structures, vol. 140, pp. 675–683, 2016, doi: 10.1016/j.compstruct.2015.12.061.

[30] H. Chang *et al.,* "Experimental study on the thermal management of an open-cathode air-cooled proton exchange membrane fuel cell stack with ultra-thin metal bipolar plates," *Energy*, vol. 263, 2023, Art. no. 125724, doi: 10.1016/j.energy.2022.125724.

[31] W. Liu *et al.,* "Performance improvement of the open-cathode proton exchange membrane fuel cell by optimizing membrane electrode assemblies," *International Journal of Hydrogen Energy*, vol. 40, no. 22, pp. 7159–7167, 2015, doi: 10.1016/j.ijhydene.2015.04.025.

[32] C. Zhao *et al.,* "Performance improvement for air-cooled open-cathode proton exchange membrane fuel cell with different design parameters of the gas diffusion layer," *Progress in Natural Science: Materials International*, vol. 30, no. 6, pp. 825–831, 2020, doi: 10.1016 /j.pnsc.2020.08.011.

[33] A. De las Heras *et al.,* "Air-cooled fuel cells: Keys to design and build the oxidant/cooling system," *Renewable Energy*, vol. 125, pp. 1–20, 2018, doi: 10.1016/j.renene.2018.02.077.

[34] T. Zeng *et al.,* "Experimental investigation on the mechanism of variable fan speed control in open cathode PEM fuel cell*," International Journal of Hydrogen Energy*, vol. 44, no. 43, pp. 24017–24027, 2019, doi: 10.1016/j.ijhydene .2019.07.119.

[35] X. Yu *et al.,* "Experimental investigation of self-regulating capability of open-cathode PEMFC under different fan working conditions," *International Journal of Hydrogen Energy*, vol. 48, no. 68, pp. 26599–26608, 2023, doi: 10. 1016/j.ijhydene.2022.06.027.

[36] C. Y. Ling *et al.,* "Compact open cathode feed system for PEMFCs," *Applied Energy*, vol. 164, pp. 670–675, 2016, doi: 10.1016/j.apenergy. 2015.12.012.

[37] L. Yin *et al.,* "Real-time thermal management of open-cathode PEMFC system based on maximum efficiency control strategy," *Asian Journal of Control*, vol. 21, no. 4, pp. 1796–1810, 2019, doi: 10.1002/asjc.2207.

[38] X. Yu *et al.,* "Thermal management of an open-cathode PEMFC based on constraint generalized predictive control and optimized strategy," *Renewable Energy*, vol. 220, 2024, Art. no. 119608, doi: 10.1016/j.renene.2023.119608.

[39] C. D'Souza *et al.,* "Thermal characteristics of an air-cooled open-cathode proton exchange membrane fuel cell stack via numerical investigation," *International Journal of Energy Research*, vol. 44, no. 14, pp. 11597–11613, 2020, doi: 10.1002/er.5785.

[40] C. Mahjoubi *et al.,* "An improved thermal control of open cathode proton exchange membrane fuel cell," *International Journal of Hydrogen Energy,* vol. 44, no. 22, pp. 11332–11345, 2019, doi: 10.1016/j.ijhydene.2018. 11.055.

[41] J. Zhou, Z. Fang, and H. Deng, "Effect of fan parameters on forced-convection open-cathode proton exchange membrane fuel cells," in *the World Hydrogen Technology Convention*, 2023, pp. 429–434, doi: 10.1007/978-981-99-8631-6_42.

[42] G. Zhang *et al.,* "Integrating full fan morphology and configuration in three-dimensional simulation of air-cooled proton exchange membrane fuel cell stack," *Fuel,* vol. 368, 2024, Art. no. 131628, doi: 10.1016/j.fuel.2024. 131628.

[43] C. Y. Ling *et al.,* "Compact open cathode feed system for PEMFCs," *Applied Energy*, vol. 164, pp. 670–675, 2016, doi: 10.1016/j.apenergy. 2015.12.012.

[44] C. Zhao *et al.,* "Air and H_2 feed systems optimization for open-cathode proton exchange membrane fuel cells," International Journal of *Hydrogen Energy*, vol. 46, no. 21, pp. 11940–11951, 2021, doi: 10.1016/j.ijhydene.2021. 01.044.

[45] J. Chen *et al.,* "Influence of cathode air supply mode on the performance of an open cathode air-cooled proton exchange membrane fuel cell stack," *Applied Thermal Engineering*, vol. 243, 2024, Art. no. 122709, doi: 10.1016/ j.applthermaleng.2024.122709.

[46] Horizon. "H-100 PEM fuel cell 100 W." Horizon Educational. Accessed: Mar. 2026. [Online.] Available: https://www.horizoneducational.com/h-100-pem-fuel-cell-100w/p1248

[47] F. Becker *et al.,* "Novel electrochemical and thermodynamic conditioning approaches and their evaluation for open cathode PEM-FC stacks," *Applied Energy*, vol. 363, 2024, Art. no. 123048, doi: 10.1016/j.apenergy.2024.123048.

[48] O. S. Süslü and I. Becerik, "On-board fuel processing for a fuel cell–heat engine hybrid system," *Energy & Fuels*, vol. 23, no. 4, pp. 1858–1873, 2009, doi: 10.1021/ef8003575.

[49] M. Hu *et al.,* "Disclosure of the internal transport phenomena in an air-cooled proton exchange membrane fuel cell—Part II: Parameter sensitivity analysis," *International Journal of Hydrogen Energy*, vol. 46, no. 35, pp. 18589–18603, 2021, doi: 10.1016/j.ijhydene.2021.03.015.

[50] G. Zhang, Z. Qu, and Y. Wang, "Full-scale three-dimensional simulation of air-cooled proton exchange membrane fuel cell stack: Temperature spatial variation and comprehensive validation," *Energy Conversion and Management*, vol. 270, 2022, Art. no. 116211, doi: 10.1016/j.enconman.2022.116211.

[51] A. P. Sasmito et al. "Computational study of forced air-convection in open-cathode polymer electrolyte fuel cell stacks," *Journal of Power Sources,* vol. 195, no. 17, pp. 5550–5563, 2010, doi: 10.1016/j.jpowsour.2010.02.083.

[52] A. Baroutaji et al., "Advancements and prospects of thermal management and waste heat recovery of PEMFC," *International Journal of Thermofluids*, vol. 9, 2021, Art. no. 100064, doi: 10.1016/j.ijft.2021.100064.

[53] Q. Wu et al., "Towards more efficient PEM fuel cells through advanced thermal management: From mechanisms to applications," *Sustainability*, vol. 17, no. 3, 2025, Art. no. 943, doi: 10.3390/su17030943.

[54] A. Pramuanjaroenkij and S. Kakaç, "The fuel cell electric vehicles: The highlight review," *International Journal of Hydrogen Energy*, vol. 48, no. 25, pp. 9401–9425, 2023, doi: 10.1016/j.ijhydene.2022.11.103.